

Wobbles and other kink-breather solutions of the sine-Gordon model

L. A. Ferreira*

Instituto de Física de São Carlos, IFSC/USP, São Carlos, São Paulo, Brazil

Bernard Piette† and Wojtek J. Zakrzewski‡

Department of Mathematical Sciences, University of Durham, Durham DH1 3LE, United Kingdom

(Received 13 August 2007; published 27 March 2008)

We study various solutions of the sine-Gordon model in (1+1) dimensions. We use the Hirota method to construct some of them and then show that the wobble, discussed in detail in a recent paper by Kälberman, is one of such solutions. We concentrate our attention on a kink and its bound states with one or two breathers. We study their stability and some aspects of their scattering properties on potential wells and on fixed boundary conditions.

DOI: [10.1103/PhysRevE.77.036613](https://doi.org/10.1103/PhysRevE.77.036613)

PACS number(s): 05.45.Yv, 81.07.De, 63.20.K–

I. INTRODUCTION

Topological solitons play an important role in the description of many phenomena in physics. In this paper we look at solitons of the simplest model in (1+1) dimensions, namely the sine-Gordon model.

This model involves a scalar field $\varphi(x, t)$ and is based on the Lagrangian density given by (we set the speed of light to $c=1$)

$$L = \frac{1}{2} \left(\frac{d\varphi}{dt} \right)^2 - \frac{1}{2} \left(\frac{d\varphi}{dx} \right)^2 - \frac{m^2}{\beta^2} [1 - \cos(\beta\varphi)]. \quad (1)$$

This particular model arises in many areas ranging from the description of Josephson junctions [2] to systems with one-dimensional dislocations [3]. The model has also been very intensively studied by mathematicians (as it describes spaces with constant negative curvature [4]) and by theoretical physicists working in integrable and conformal field theories [5].

As is well known [6] the model possesses kink, antikink, and breather solutions. A kink solution is a static field configuration which solves the Euler Lagrange equations based on (1), i.e.,

$$\varphi_{tt} - \varphi_{xx} = -\frac{m^2}{\beta} \sin(\beta\varphi), \quad (2)$$

and satisfies the boundary conditions $\varphi(x=-\infty)=0$ and $\beta\varphi(x=\infty)=2\pi$. Such a field is well known [6] and is given by

$$\varphi = \frac{4}{\beta} \arctan\{\exp[m(x-x_0)]\}. \quad (3)$$

For the antikink the boundary conditions are interchanged and in the field configuration given above there is a $-$ sign before $(x-x_0)$.

In addition, the model possesses also so-called breather solutions. These are nonstatic field solutions of (2) given by

$$\varphi = \frac{4}{\beta} \arctan\left(\frac{\sqrt{1-\omega^2} \sin(m\omega t)}{\omega \cosh[m\sqrt{1-\omega^2}(x-x_0)]} \right). \quad (4)$$

Here ω is a free parameter of the solution which varies from -1 to 1 . The breather field, which can be thought of as describing a bound state of a kink and an antikink, oscillates with frequency $m\omega$.

As the basic Lagrangian is Lorentz covariant, all these field configurations can be Lorentz boosted, resulting in field configurations moving with velocity $v < c=1$.

Recently, there has been some controversy as to whether a kink possesses an internal mode [7,8]. Such a mode was claimed to exist by Boesch and Willis [9] and then disputed by Quintero *et al.* [10]. The mode at stake is a possible internal mode of zero frequency which may have arisen in numerical studies of the sine-Gordon model. Such a mode could be a genuine oscillatory mode or a numerical artifact.

In fact, as is well known [6], the sine-Gordon model possesses many solutions in addition to the above mentioned kinks and breathers. One such solution was recently studied extensively by Kälberman [1]. He called it a “wobble” and looked at its properties in detail. However, it is not clear from his discussion whose claims his wobble solution supports.

It is worth recalling at this stage that the wobble is only one of many solutions involving a kink with breathers. Hence we have decided to reconsider this subject and look in some detail at these solutions. In particular, we have decided to present explicit forms of the field configurations that describe some of these solutions, so that they become better known outside the integrable model community. We have also decided to look at some of their properties, paying particular attention to their stability and their scattering properties on defects (here taken in the form of an interaction with potential holes and boundaries). This we discuss in the next sections.

II. THE WOBBLE

The wobble solution of Kälberman [1] involves a field configuration describing a static kink and a breather. In his

*laf@ifsc.usp.br

†B.M.A.G.Piette@durham.ac.uk

‡W.J.Zakrzewski@durham.ac.uk

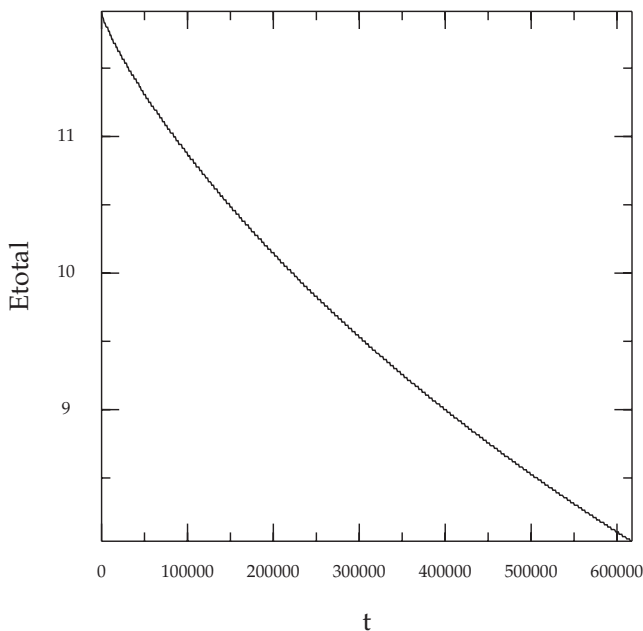


FIG. 1. Energy as a function of time as seen in a simulation started with $\lambda=1.15$

paper Kälbermann gives an analytic form of this solution, obtained by using the inverse scattering method of Lamb and Segur, and then discusses some of its properties.

In our work we use the Hirota method [11] of deriving such solutions as discussed in detail in Appendix A. We derive in Appendix A 4 the exact solution describing a kink and a breather moving with respect to each other. The solution is given by Eq. (A21). However, the wobble corresponds to a kink and a breather sitting one on top of the other and not having a relative motion. Therefore, if one sets the the velocities to zero in the general solution (A21) one gets the wobble solution as

$$\varphi = \frac{4}{\beta} \arctan \frac{\left(\frac{\sqrt{1-\omega^2}}{\omega} \sin(m\omega t) + \frac{1}{2} e^{\varepsilon m x} (e^{-m\sqrt{1-\omega^2}x} + \rho^2 e^{m\sqrt{1-\omega^2}x}) \right)}{\left(\cosh(m\sqrt{1-\omega^2}x) + \frac{\sqrt{1-\omega^2}}{\omega} \rho e^{\varepsilon m x} \sin(m\omega t) \right)}, \quad (5)$$

where ω is a frequency varying from -1 to 1 , and

$$\rho = \frac{1 - \varepsilon \sqrt{1 - \omega^2}}{1 + \varepsilon \sqrt{1 - \omega^2}}, \quad (6)$$

where $\varepsilon = \pm 1$ corresponds to the kink (+1) or antikink (-1).

This agrees with the expression given by Kälbermann. As is clear from (5) the field configuration depends on one parameter (the frequency of the breather), and so we have studied the stability of this field configuration by calculating φ and its time derivative from (5) and then used the fourth-order Runge-Kutta method to simulate the time evolution of this configuration (the spatial derivatives were calculated using central differences). Our simulations involved looking at a breather-kink system ($\varepsilon=1$) and for β and m we took β

$=2$, $m=1$. Hence, for the kink φ varies from 0 to π . In fact we used this choice of β and m in all our simulations. The results of our simulations were in complete agreement with the analytical expression, thus showing that the solution is stable with respect to small perturbations (due to the discretizations).

Next we tried to assess the stability of the wobble with respect to larger perturbations. We performed several perturbations, the most important of them being the perturbation of the original slope of the kink [i.e., in the expression (5) we have replaced $\exp(\varepsilon m x)$ by $\exp(\lambda x)$ where $\lambda \neq 1$]. We have performed numerical simulations with $\lambda=1.05$, 1.15 , 1.18 , 1.20 , 1.24 , and 1.3 .

Each perturbation added an extra energy to the system. Such a system was then unstable and so it evolved toward a stable wobble, emitting some radiation which was sent out toward the boundaries of the grid. To prevent reflections from the boundaries, we absorbed the energy there. For λ close to 1 —the perturbations were small—the system returned to its initial configuration (with $\lambda=1.0$). For larger values of the perturbation the system was more perturbed and often not only kept on sending out its excess of energy but also, at regular intervals, altered its frequency of oscillation (increasing it) which allowed it to send out even more radiation. In Fig. 1 we present plots of the time dependence of the total energy as seen in the simulation in which λ was set at 1.15 .

We have also studied the case of $v=v_k=v_B \neq 0$. In this case we had a system consisting of a kink and a breather moving with a constant velocity. Again, the system was stable (we run it with very small v to avoid having problems with the boundaries and for larger values of v with fixed boundary conditions).

Then we performed a series of simulations in which the initial configuration was sent toward a potential hole. This was achieved by making $\alpha \equiv \frac{m^2}{\beta^2}$ in (1) x dependent; i.e., we set

$$\alpha(x) = \begin{cases} 1 & \text{for } |x| > 5, \\ \alpha_0 < 1 & \text{for } -5 < x < 5. \end{cases} \quad (7)$$

Then by placing the breather and the kink far away from the hole (i.e., from $-5 < x < 5$), and sending them toward it we could study the effects of their scattering on the hole.

In Fig. 2 we exhibit the field configurations (at two values of time) seen in one such simulation. The simulation involved placing the breather around $x \sim -30$, and the kink around $x \sim -20$, and sending them with velocity $v=0.05$ toward the hole of depth 0.1 located between -15 and 15 . In Fig. 2(a) we show the field configurations at $t=60$, i.e., just before the kink reached the hole. When in the hole the breather separated and one of its constituents (the kink) remained trapped in it, oscillating back and forth, while the original kink and the antikink from the breather emerged at the other side of the hole. This is clearly seen in Fig. 2(b), which shows the field configuration at $t=450$. Other simulations produced other equally interesting results (often involving splitting of the breather).

We also found that the hole can separate the breather from the kink (in one simulation we saw the kink being trapped in the hole while the breather bounced off the kink trapped in the hole and has returned to its original position). As studied by two of us [12], the scattering of a breather on the hole is very complicated and produces many different outcomes; this time we have even more possibilities and so we have decided to postpone the further study of this problem to some future work.

III. KINK AND TWO BREATHERS

In this section we briefly discuss another interesting solution of the sine-Gordon model; namely, the solution corre-

sponding to one static kink and two breathers.

In this case, as shown in the Appendix, the field is given, for $\beta=m=1$, by

$$\varphi = 4 \arctan \frac{A}{B}, \quad (8)$$

where

$$\begin{aligned} \mathcal{A} = & -2 \cotan \theta_1 e^{x \cos \theta_1} \sin(t \sin \theta_1) - 2 \cotan \theta_2 e^{x \cos \theta_2} \sin(t \sin \theta_2) + e^x - 2 \cotan \theta_2 \sigma_{12}^{(+)} \sigma_{12}^{(-)} e^{x(2 \cos \theta_1 + \cos \theta_2)} \sin(t \sin \theta_2) \\ & + \rho_1^2 e^{2x \cos \theta_1} e^x - 2 \cotan \theta_1 \sigma_{12}^{(+)} \sigma_{12}^{(-)} e^{x(\cos \theta_1 + 2 \cos \theta_2)} \sin(t \sin \theta_1) + \rho_2^2 e^{2x \cos \theta_2} e^x \\ & + 2 \sigma_{12}^{(-)} \rho_1 \rho_2 \cotan \theta_1 \cotan \theta_2 e^{x(\cos \theta_1 + \cos \theta_2)} \cos[t(\sin \theta_1 + \sin \theta_2)] \\ & - 2 \sigma_{12}^{(+)} \rho_1 \rho_2 \cotan \theta_1 \cotan \theta_2 e^{x(\cos \theta_1 + \cos \theta_2)} \cos[t(\sin \theta_1 - \sin \theta_2)] + (\sigma_{12}^{(+)} \sigma_{12}^{(-)} \rho_1 \rho_2)^2 e^{2x(\cos \theta_1 + \cos \theta_2)} \end{aligned} \quad (9)$$

and

$$\begin{aligned} \mathcal{B} = & 1 + e^{2x \cos \theta_1} + e^{2x \cos \theta_2} + 2 \rho_1 \cotan \theta_1 e^{x \cos \theta_1} \sin(t \sin \theta_1) + 2 \rho_2 \cotan \theta_2 e^{x \cos \theta_2} \sin(t \sin \theta_2) \\ & + 2 \sigma_{12}^{(-)} \cotan \theta_1 \cotan \theta_2 e^{x(\cos \theta_1 + \cos \theta_2)} \cos[t(\sin \theta_1 + \sin \theta_2)] - 2 \sigma_{12}^{(+)} \cotan \theta_1 \cotan \theta_2 e^{x(\cos \theta_1 + \cos \theta_2)} \cos[t(\sin \theta_1 - \sin \theta_2)] \\ & + (\sigma_{12}^{(+)} \sigma_{12}^{(-)})^2 e^{2x(\cos \theta_1 + \cos \theta_2)} + 2 \sigma_{12}^{(+)} \sigma_{12}^{(-)} \rho_1^2 \rho_2 \cotan \theta_2 e^{x(2 \cos \theta_1 + \cos \theta_2)} \sin(t \sin \theta_2) \\ & + 2 \sigma_{12}^{(+)} \sigma_{12}^{(-)} \rho_1 \rho_2^2 \cotan \theta_1 e^{x(\cos \theta_1 + 2 \cos \theta_2)} \sin(t \sin \theta_1). \end{aligned} \quad (10)$$

Here

$$\rho_i = -\frac{1 - \cos \theta_i}{1 + \cos \theta_i}, \quad \sigma_{12}^{(\pm)} = -\frac{1 - \cos(\theta_1 \pm \theta_2)}{1 + \cos(\theta_1 \pm \theta_2)}. \quad (11)$$

This solution depends on two constants (θ_1, θ_2), which control the frequencies of the breather oscillations.

We have tested the stability of this solution by using the expression (8) to calculate $\varphi(t=0)$ and $\frac{d\varphi}{dt}(t=0)$ and then performing a numerical simulation of (2). As before, the discretization has produced a small perturbation but the field configuration was stable; i.e., after a long simulation (we run it until $t=5000$) the field was indistinguishable from the expression (8) and there was no noticeable radiation. Hence we can conclude that this field configuration is also stable.

IV. PERTURBED FIELD CONFIGURATIONS

Given that we have many field configurations that resemble perturbed kinks (i.e., that are given by kinks and breathers), we have tried to see what happens when one perturbs a kink and lets it evolve in time. We looked at various perturbations, paying particular attention to configurations which involved adding to a kink an extra perturbation of the form

$$\delta\varphi(t=0) = \frac{B}{\cosh(\mu x)}, \quad \delta\frac{\partial\varphi}{\partial t}(t=0) = \frac{A}{\cosh(\nu x)}. \quad (12)$$

We looked at various values of A, B, μ , and ν . In all cases the perturbation made the kink move and generated many moving breatherlike configurations. We let the system evolve—absorbing the energy at the boundaries of our grid. This had the effect of slowing down the kink. In Fig. 3 we present plots of the total energy, and of the potential energy, of one such simulation (corresponding to the values $A=0.5, B=0.5, \mu=1.0$, and $\nu=0.2$). The curve in Fig. 3(a) shows a steady decrease in total energy down to close to the value of the energy of one stationary kink.

We note some steps of the decrease of the total energy (they correspond to the moments when the kink was reflected from the boundaries). The potential has also gradually settled as seen from the plot. Its oscillation demonstrates the existence of transient time-dependent structures (i.e., breathers). This can be seen from looking at the time dependence of individual field configurations. In Fig. 4, we present plots of the fields at $t=6750$ and 6753 . They show many breatherlike structures—the clearest ones being close to $x=35$ and -38 .

Thus it is clear to us that a general field configuration will gradually split into moving kinks and breathers and some radiation, which will quickly move out to the boundaries.

However, the resultant field configuration is metastable; it still radiates, albeit very slowly, and gradually evolves toward a field configuration involving mainly a kink. Whether at the end of its evolution we end up with a kink or a kink with some breathers is hard to determine.

V. THE ENERGY

In this section we give a simple formula for the energy of the exact solutions considered in this paper. The energy for all the solutions coming from the Hirota method is easy to calculate since, as we show below, it comes from surface terms. In addition, the energy is additive for the nonlinear Hirota superposition of solutions. The Hamiltonian density for the sine-Gordon theory (1) is given by

$$H = \frac{1}{2}(\partial_t \varphi)^2 + \frac{1}{2}(\partial_x \varphi)^2 + \frac{2m^2}{\beta^2} \left[\sin\left(\frac{1}{2}\beta\varphi\right) \right]^2. \quad (13)$$

Replacing the field φ in terms of the Hirota τ functions as given in Appendix A, Eq. (A1), we get

$$H = -\frac{1}{\beta^2} \left[\left(\frac{\partial_+ \tau_1}{\tau_1} - \frac{\partial_+ \tau_0}{\tau_0} \right)^2 + \left(\frac{\partial_- \tau_1}{\tau_1} - \frac{\partial_- \tau_0}{\tau_0} \right)^2 + \frac{m^2}{2} \left(\frac{\tau_0}{\tau_1} - \frac{\tau_1}{\tau_0} \right)^2 \right]. \quad (14)$$

However, this expression can be rewritten as

$$H = \frac{1}{\beta^2} (\partial_+ - \partial_-)^2 (\ln \tau_0 + \ln \tau_1) + H_{\text{cor}}, \quad (15)$$

where

$$H_{\text{cor}} = -\frac{1}{\beta^2} \left(\frac{\partial_+^2 \tau_0}{\tau_0} + \frac{\partial_-^2 \tau_0}{\tau_0} + \frac{\partial_+^2 \tau_1}{\tau_1} + \frac{\partial_-^2 \tau_1}{\tau_1} - 2 \frac{\partial_+ \tau_1}{\tau_1} \frac{\partial_+ \tau_0}{\tau_0} - 2 \frac{\partial_- \tau_1}{\tau_1} \frac{\partial_- \tau_0}{\tau_0} \right). \quad (16)$$

The solutions obtained by the Hirota ansatz (A4) satisfy, in addition to the Hirota equations (A3), also the additional equations

$$\tau_1 \partial_+^2 \tau_0 + \tau_0 \partial_-^2 \tau_1 - 2 \partial_+ \tau_0 \partial_- \tau_1 = 0. \quad (17)$$

This fact is proved, in a much more general setting, in Ref. [13]. In fact, it is shown there that all solutions that can be obtained from the vacuum solution $\varphi=0$ by the dressing transformations satisfy (17). The Hirota solutions are, of course, of this type. Therefore, it turns out that for these solutions one has $H_{\text{cor}}=0$, and so

$$H = \frac{4}{\beta^2} \partial_x^2 (\ln \tau_0 + \ln \tau_1), \quad (18)$$

where we have used the fact that $(\partial_+ - \partial_-) = 2\partial_x$ [see (A2)]. Therefore, the energy becomes

$$E = \int_{-\infty}^{\infty} dx H = \frac{4}{\beta^2} \partial_x (\ln \tau_0 + \ln \tau_1) \Big|_{x=-\infty}^{x=\infty} \quad (19)$$

and so is determined entirely by the asymptotic values of the τ_i functions.

In fact, this result (in a different and less explicit form) has been known for a while for kinks and antikinks, to people working in integrable and conformal field theories [14,15]. Here we have presented it in a form that is more explicit and more easily accessible to people working in other areas of physics. For more details of the general proof, see [13].

Looking at the solutions in the N -soliton sector, given in (A6), one observes that the asymptotic behavior of the τ function is determined by the exponentials of the Γ_i 's given in (A5), i.e.,

$$\Gamma_i = \frac{m}{2} \left[\left(z_i + \frac{1}{z_i} \right) x + \left(z_i - \frac{1}{z_i} \right) t \right]. \quad (20)$$

In (19) we have to evaluate the quantities $\frac{\partial_x \tau_\alpha}{\tau_\alpha} \Big|_{x=\pm\infty}$. Therefore, if a given combination of exponentials of the Γ_i 's dominates the numerator of $\frac{\partial_x \tau_\alpha}{\tau_\alpha}$, for $x \rightarrow \pm\infty$, then the same combination dominates the denominator. Consequently, when the limit $x \rightarrow \pm\infty$ is taken, we are left with the ratio of these two dominant terms, which are equal except for the constant term (in the numerator) coming from the x derivative of the exponentials, i.e., terms of the form $\frac{m}{2} (z_i + \frac{1}{z_i})$. Therefore, the contribution to (19) is just the terms from the x derivatives. In addition, τ_0 and τ_1 , given in (A6), have the same form except for the minus signs, and so their contributions to (19) are equal, despite these minus signs, which cancel when the limit $x \rightarrow \pm\infty$ is taken.

Notice that the solution (A6) contains all possible combinations of the exponentials of the Γ_i 's, such that each Γ_i appears at most once. Therefore, it is clear that the dominant exponential in the limit $x \rightarrow +\infty$ is $\exp(\sum_i \Gamma_i)$, where in the sum we include all Γ_i 's such that $\text{Re}(z_i + \frac{1}{z_i}) > 0$. Similarly, the dominant exponential in the limit $x \rightarrow -\infty$ is $\exp(\sum_i \Gamma_i)$, where the sum involves all Γ_i 's such that $\text{Re}(z_i + \frac{1}{z_i}) < 0$. Thus, the energy depends only on the modulus of $\text{Re}(z_i + \frac{1}{z_i})$. The parameters z_i can be complex for some solutions and so, writing them as $z_i = e^{-\alpha_i + i\theta_i}$, one gets

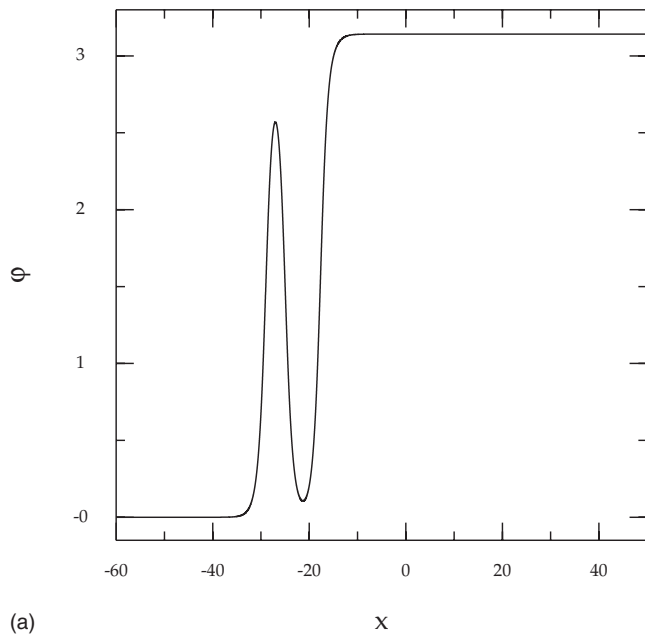
$$z_i + \frac{1}{z_i} = 2(\cos \theta_i \cosh \alpha_i - i \sin \theta_i \sinh \alpha_i). \quad (21)$$

Thus we conclude that the energy (19) for the solutions (A6), is given by

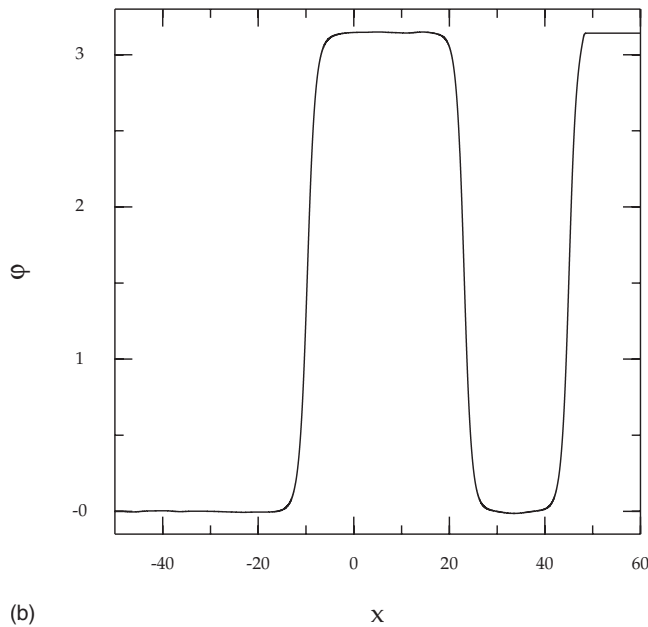
$$E = \frac{8m}{\beta^2} \sum_{i=1}^N (|\cos \theta_i| \cosh \alpha_i - i \sin \theta_i \sinh \alpha_i), \quad (22)$$

where N corresponds to the N -soliton sector in which the solution lies. The energy will then be real for some special choices of the parameters z_i . But whenever this happens the energy is automatically positive. Of course, the energy is real whenever the solution φ is real.

The energies for the solutions we consider in this paper are then given by (1) for the one-soliton constructed in Appendix A 2,



(a)



(b)

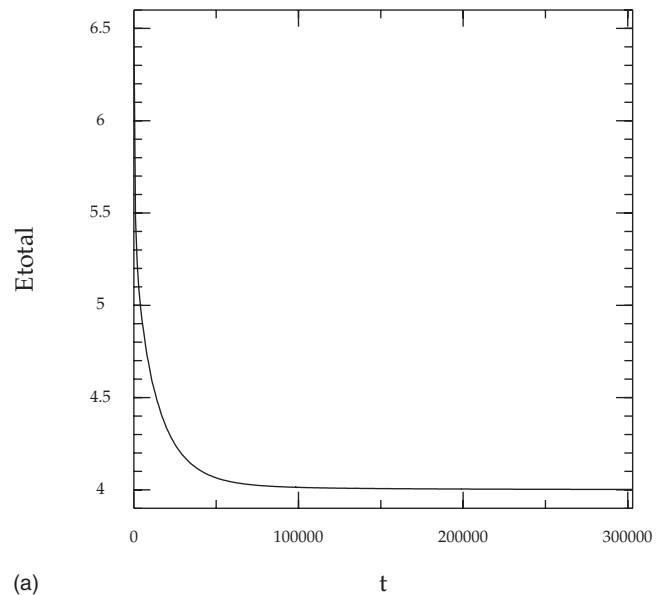
FIG. 2. Field configurations seen in a simulation involving a wobble scattering on a potential hole (of depth 0.1 and located in $-15 < x < 15$). $t =$ (a) 60 and (b) 450.

$$E_{\text{one-soliton}} = \frac{8m}{\beta^2} \frac{1}{\sqrt{1-v^2}}; \quad (23)$$

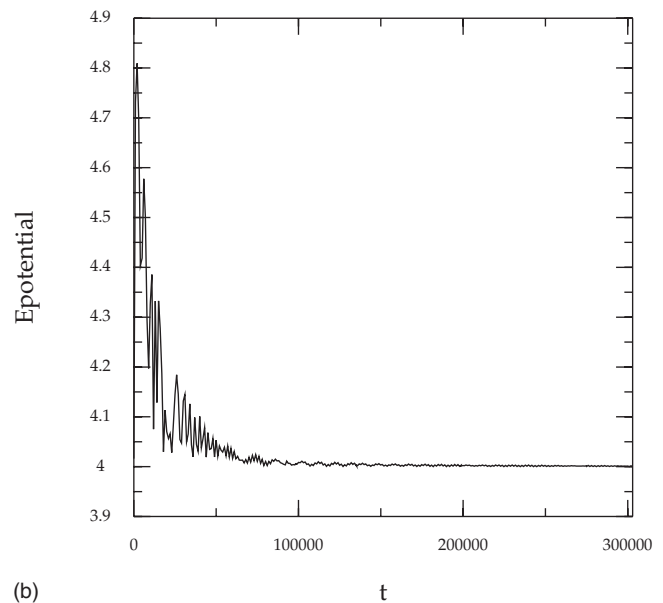
(2) for the breather constructed in Appendix A 3,

$$E_{\text{breather}} = \frac{16m}{\beta^2} \frac{\sqrt{1-\omega^2}}{\sqrt{1-v^2}}; \quad (24)$$

(3) for the wobble constructed in Sec. II and Appendix A 4,



(a)



(b)

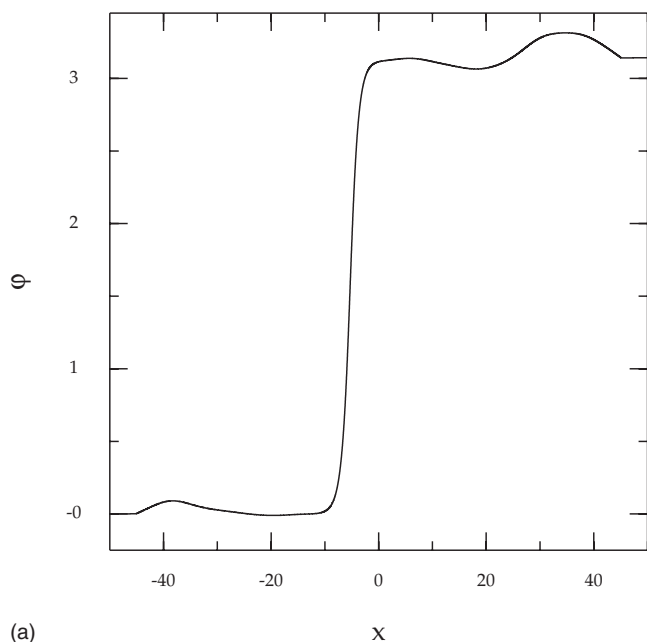
FIG. 3. Energies as a function of time as seen when the starting file was given by (12): (a) total and (b) potential energy.

$$E_{\text{wobble}} = \frac{8m}{\beta^2} \frac{1}{\sqrt{1-v_K^2}} + \frac{16m}{\beta^2} \frac{\sqrt{1-\omega^2}}{\sqrt{1-v_B^2}}; \quad (25)$$

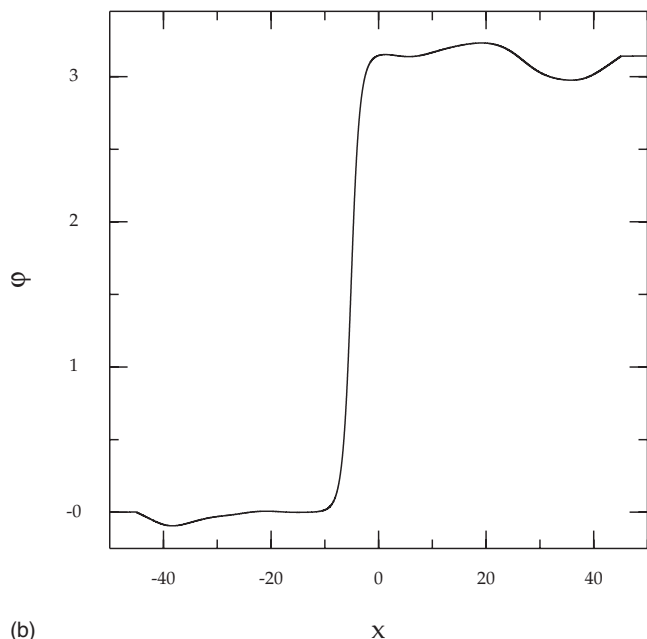
and (4) for the solution of the kink with two breathers constructed in Sec. III and Appendix A 5 (with their velocities set to zero),

$$E_{\text{kink+two breathers}} = \frac{8m}{\beta^2} + \frac{16m}{\beta^2} \sqrt{1-\omega_1^2} + \frac{16m}{\beta^2} \sqrt{1-\omega_2^2}, \quad (26)$$

where $\omega_i = \sin \theta_i$, $i=1,2$.



(a)



(b)

FIG. 4. Field configurations at $t =$ (a) 6750 and (b) 6753.

VI. FINAL REMARKS

In this paper we have drawn the attention of the readers to the rich structure of solutions (of finite energy) of the sine-Gordon model. Even in the one-kink sector there are solutions involving, in addition to the kink, also many breathers. As the energy of each breather depends on its frequency (and vanishes in the limit of this frequency going to 1) the extra energy, due to these extra breathers, does not have to be very large. The solutions appear to be stable, and this stability is guaranteed by the integrability of the model. We have tested this numerically and have found that small perturbations, due to the discretizations, do not alter this stability. To change it we need something more drastic—like the absorption or the

space variation of the potential (i.e., the coefficient of the sine term in the Lagrangian). But even then the effects are not very large—one sees splitting of breathers, etc. but no “global annihilation.”

At the same time we have looked at the total energy and the energy density of a general solution. We point out that the total energy is determined by the asymptotic values of the fields [i.e., is given by (19)]. This result was known earlier (for kinks and antikinks) to people working in integrable and conformal field theories but may not be known generally. We have given a general proof of this in a separate, rather technical, paper [13], but we have also checked it explicitly for all field configurations involving up to five kinks (or anti-kinks).

Our results do not answer, definitively, the question as to whether or not a kink possesses an internal mode of oscillation. The perturbation of the kink we performed in Sec. IV did not produce any oscillatory internal mode. On the contrary, all the energy given to the kink by the perturbation was used to produce breatherlike excitations, which died away very slowly. In fact, the extremely slow decay of these excitations indicates the difficulty of settling the issue of the existence of the internal mode. If simulations are not done very carefully and run for very long times, then this fact can lead to incorrect interpretations.

As we have pointed out, one can get oscillatory kink configurations by constructing exact solutions corresponding to the stationary superposition of a kink and one or many breathers. Such a case of a kink and a breather was named a wobble by Kälbermann [1]. In the case of the wobble the frequency of oscillation cannot be greater than 1, and the energy of the oscillation goes to zero as the frequency approaches 1. Boesch and Willis [9] claimed to have seen an oscillatory mode of this kink just above the phonon band, i.e., just above 1. If that is so, the wobble does not correspond to that mode. It is true, however, that the frequency of the wobble can go above 1 by a Lorentz boost. One has then to settle the issue of whether the simulations of Boesch and Willis were precise enough to separate this effect. If one considers the exact stationary superposition of a kink and two breathers one can get frequencies of oscillations greater than 1, as shown in (8). However, this is in a context different from that discussed in the literature, where the considered frequencies are studied in the linear approximation. Hence we feel that it is extremely likely that the mode seen by Boesch and Willis is in reality some sort of linear combination of various modes involving breathers and a kink but, strictly speaking, we have not been able to prove this. In addition, although our simulations have shown that the kink plus breathers are stable solutions against the discretization, they can be pulled apart by scattering through a hole, as mentioned at the end of Sec. II. The fact that a kink solution of the equations of motion can involve many breathers makes the problem of the zero mode difficult to resolve analytically (and in the literature it is discussed only in the linear approximation) and almost impossible to resolve numerically. The rich spectrum of the solutions and the appearance of many breathers makes this task particularly hard to perform. It would be interesting to see whether these extra breathers play a significant role in any physical applications of the model.

ACKNOWLEDGMENTS

W.J.Z. was supported by a grant from FAPESP which is gratefully acknowledged. W.J.Z. also wishes to thank the University of São Paulo in São Carlos for its hospitality and Gilberto Nakamura for the help with computers in São Carlos. We all thank Professor F. C. Alcaraz for the use of the computer facilities.

APPENDIX

1. Hirota's method

In order to solve the sine-Gordon equation (2) by the Hirota method we introduce the Hirota τ function as

$$\varphi = \frac{2i}{\beta} \ln \frac{\tau_1}{\tau_0}. \tag{A1}$$

Using light-cone coordinates

$$x_{\pm} = \frac{1}{2}(t \pm x), \quad \partial_{\pm} = \partial_t \pm \partial_x, \quad \partial^2 = \partial_t^2 - \partial_x^2 = \partial_+ \partial_-, \tag{A2}$$

and replacing (A1) into (2), we get

$$\begin{aligned} & \frac{\partial_+ \partial_- \tau_0}{\tau_0} - \frac{\partial_+ \tau_0 \partial_- \tau_0}{\tau_0^2} - \frac{m^2}{4} \left[\left(\frac{\tau_1}{\tau_0} \right)^2 - 1 \right] \\ & = \frac{\partial_+ \partial_- \tau_1}{\tau_1} - \frac{\partial_+ \tau_1 \partial_- \tau_1}{\tau_1^2} - \frac{m^2}{4} \left[\left(\frac{\tau_0}{\tau_1} \right)^2 - 1 \right]. \end{aligned}$$

Requiring both sides to vanish, we get the Hirota equations for the sine-Gordon model:

$$\tau_0 \partial_+ \partial_- \tau_0 - \partial_+ \tau_0 \partial_- \tau_0 + \frac{m^2}{4} (\tau_0^2 - \tau_1^2) = 0,$$

$$\tau_1 \partial_+ \partial_- \tau_1 - \partial_+ \tau_1 \partial_- \tau_1 + \frac{m^2}{4} (\tau_1^2 - \tau_0^2) = 0. \tag{A3}$$

The solutions of (A3) are obtained by the Hirota ansatz

$$\begin{aligned} \tau_{\alpha} = 1 + \varepsilon \sum_{i=1}^N b_i^{(\alpha)} e^{\Gamma_i} + \varepsilon^2 \sum_{i,j=1}^N b_{ij}^{(\alpha)} e^{\Gamma_i + \Gamma_j} + \varepsilon^3 \sum_{i,j,k=1}^N b_{ijk}^{(\alpha)} e^{\Gamma_i + \Gamma_j + \Gamma_k} \\ + \dots, \quad \alpha = 0, 1, \end{aligned} \tag{A4}$$

where

$$\Gamma_i = m \left(z_i x_+ - \frac{x_-}{z_i} \right) \tag{A5}$$

and where z_i are arbitrary (complex) parameters. Replacing (A4) into (A3) and expanding in powers of ε , one obtains the coefficients $b^{(\alpha)}$ recursively. The series in (A4) truncates at order N , leading to an exact solution given by

$$\begin{aligned} \tau_{\alpha} = 1 + (-1)^{\alpha} \sum_{l=1}^N a_l e^{\Gamma(z_l)} + \sum_{l_1 < l_2 = 1}^N \left(\frac{z_{l_1} - z_{l_2}}{z_{l_1} + z_{l_2}} \right)^2 a_{l_1} a_{l_2} e^{\Gamma(z_{l_1}) + \Gamma(z_{l_2})} + \dots + (-1)^{\alpha} \\ \times \sum_{l_1 < l_2 < l_3 = 1}^N \left(\frac{z_{l_1} - z_{l_2}}{z_{l_1} + z_{l_2}} \right)^2 \left(\frac{z_{l_1} - z_{l_3}}{z_{l_1} + z_{l_3}} \right)^2 \left(\frac{z_{l_2} - z_{l_3}}{z_{l_2} + z_{l_3}} \right)^2 a_{l_1} a_{l_2} a_{l_3} e^{\Gamma(z_{l_1}) + \Gamma(z_{l_2}) + \Gamma(z_{l_3})} \dots + (-1)^{\alpha N} \prod_{k_1 < k_2 = 1}^N \left(\frac{z_{k_1} - z_{k_2}}{z_{k_1} + z_{k_2}} \right)^2 \prod_{l=1}^N a_l e^{\Gamma(z_l)} \end{aligned} \tag{A6}$$

where a_i are arbitrary parameters.

2. The one-soliton solutions

The one-soliton solutions correspond to $N=1$ and the following choice of parameters in (A6):

$$a_1 = i e^{-\varepsilon \gamma x_0}, \quad z_1 = \varepsilon e^{-\alpha}, \quad \varepsilon = \pm 1, \quad \alpha \text{ real.} \tag{A7}$$

Then the arguments of the exponentials become

$$\Gamma_1 = \varepsilon \gamma (x - vt), \quad \gamma = m \cosh \alpha = \frac{m}{\sqrt{1 - v^2}}, \quad v = \tanh \alpha. \tag{A8}$$

Therefore, (A1) and (A6) give

$$\varphi = \frac{4}{\beta} \arctan \exp[\varepsilon \gamma (x - vt - x_0)]. \tag{A9}$$

3. The breather solution

The breather solution lies in the two-soliton sector, and it is obtained by taking $N=2$, and the following choice of parameters in (A6):

$$z_1 = e^{-\alpha + i\theta}, \quad z_2 = z_1^*, \quad a_1 = i \frac{e^{\eta + i\xi}}{\tan \theta}, \quad a_2 = -a_1^*. \tag{A10}$$

Then we have that $\Gamma_2 = \Gamma_1^*$ and introducing $\tilde{\Gamma}_1 = \Gamma_1 + \eta + i\xi$ we obtain

$$\tilde{\Gamma}_1 = \Gamma_R + i\Gamma_I \tag{A11}$$

with

$$\Gamma_R = \frac{m \cos \theta}{\sqrt{1-v^2}}(x-vt) + \eta, \quad \Gamma_I = \frac{m \sin \theta}{\sqrt{1-v^2}}(t-vx) + \xi \tag{A12}$$

and

$$v = \tanh \alpha. \tag{A13}$$

Thus

$$\varphi = \frac{4}{\beta} \arctan \frac{(\cotan \theta) \cos \Gamma_I}{\cosh \Gamma_R}. \tag{A14}$$

If one now takes

$$\eta = v = 0, \quad \xi = \frac{\pi}{2}, \quad \omega \equiv \sin \theta, \quad -\frac{\pi}{2} \leq \theta \leq \frac{\pi}{2},$$

one gets

$$\varphi = \frac{4}{\beta} \arctan \left(\frac{\sqrt{1-\omega^2}}{\omega} \frac{\sin(m\omega t)}{\cosh(m\sqrt{1-\omega^2}x)} \right). \tag{A15}$$

4. The wobble or the kink with a breather

To have a configuration describing a kink with a breather we take the following values for the parameters of the three-soliton solution ($N=3$) in (A6)

$$z_1 = e^{-\alpha_B + i\theta}, \quad z_2 = z_1^*, \quad z_3 = \varepsilon e^{-\alpha_K},$$

$$a_1 = i \frac{e^{\eta_B + i\xi_B}}{\tan \theta}, \quad a_2 = -a_1^*, \quad a_3 = i e^{\eta_K}. \tag{A16}$$

Then one gets

$$\tilde{\Gamma}_3 = \varepsilon \gamma_K (x - v_K t) + \eta_K, \quad \gamma_K = m \cosh \alpha_K, \quad v_K = \tanh \alpha_K, \tag{A17}$$

and again one has $\Gamma_2 = \Gamma_1^*$. Then introducing $\tilde{\Gamma}_1 = \Gamma_1 + \eta_B + i\xi_B$, one obtains

$$\varphi = \frac{4}{\beta} \arctan \frac{\left(\frac{\sqrt{1-\omega^2}}{\omega} \sin(m\omega t) + \frac{1}{2} e^{\varepsilon m x} (e^{-m\sqrt{1-\omega^2}x} + \rho^2 e^{m\sqrt{1-\omega^2}x}) \right)}{\left(\cosh(m\sqrt{1-\omega^2}x) + \frac{\sqrt{1-\omega^2}}{\omega} \rho e^{\varepsilon m x} \sin(m\omega t) \right)}. \tag{A23}$$

5. The kink with two breathers

To get a field configuration describing a kink and two breathers that are all at rest and located at the same position, we take the parameters of the five-soliton solution ($N=5$) in (A6) as

$$\tilde{\Gamma}_1 = \Gamma_R + i\Gamma_I \tag{A18}$$

with

$$\Gamma_R = \frac{m}{\sqrt{1-v_B^2}} \cos \theta (x - v_B t) + \eta_B,$$

$$\Gamma_I = \frac{m}{\sqrt{1-v_B^2}} \sin \theta (t - v_B x) + \xi_B,$$

and $v_B = \tanh \alpha_B$. Next we define

$$\left(\frac{z_1 - z_3}{z_1 + z_3} \right)^2 = \rho e^{i\phi} \tag{A19}$$

with

$$\rho = \frac{\cosh(\alpha_B - \alpha_K) - \varepsilon \cos \theta}{\cosh(\alpha_B - \alpha_K) + \varepsilon \cos \theta} \tag{A20}$$

and

$$\phi = 2 \arctan \frac{\varepsilon \sin \theta}{\sinh(\alpha_B - \alpha_K)}.$$

Then

$$\varphi = \frac{4}{\beta} \arctan \frac{[2(\cotan \theta) \cos \Gamma_I + e^{\tilde{\Gamma}_3} (e^{-\Gamma_R} + \rho^2 e^{\Gamma_R})]}{[(e^{-\Gamma_R} + e^{\Gamma_R}) - 2(\cotan \theta) \rho e^{\tilde{\Gamma}_3} \cos(\Gamma_I + \phi)]}. \tag{A21}$$

If one now takes

$$\eta_K = \eta_B = v_B = v_K = 0, \quad \xi_B = \frac{\pi}{2},$$

and denotes

$$\omega \equiv \sin \theta, \quad -\frac{\pi}{2} \leq \theta \leq \frac{\pi}{2},$$

then

$$\rho = \frac{1 - \varepsilon \sqrt{1-\omega^2}}{1 + \varepsilon \sqrt{1-\omega^2}}, \quad \phi = \pm \pi, \tag{A22}$$

and so

$$z_1 = e^{i\theta_1}, \quad z_2 = z_1^*, \quad z_3 = e^{i\theta_2}, \quad z_4 = z_3^*, \quad z_5 = \varepsilon, \tag{A24}$$

and

$$a_1 = -a_2 = -\cotan \theta_1, \quad a_3 = -a_4 = -\cotan \theta_2, \quad a_5 = i. \quad (\text{A25})$$

Then, setting $m = \beta = 1$, one gets

$$\Gamma_1 = \Gamma_2^* = x \cos \theta_1 + it \sin \theta_1, \quad (\text{A26})$$

$$\Gamma_3 = \Gamma_4^* = x \cos \theta_2 + it \sin \theta_2, \quad \Gamma_5 = \varepsilon x.$$

In addition, we have

$$\left(\frac{z_1 - z_2}{z_1 + z_2}\right)^2 = -\tan^2 \theta_1, \quad \left(\frac{z_3 - z_4}{z_4 + z_4}\right)^2 = -\tan^2 \theta_2,$$

$$\left(\frac{z_1 - z_5}{z_1 + z_5}\right)^2 = \left(\frac{z_2 - z_5}{z_2 + z_5}\right)^2 = -\frac{1 - \varepsilon \cos \theta_1}{1 + \varepsilon \cos \theta_1} \equiv \rho_1,$$

$$\left(\frac{z_3 - z_5}{z_3 + z_5}\right)^2 = \left(\frac{z_4 - z_5}{z_4 + z_5}\right)^2 = -\frac{1 - \varepsilon \cos \theta_2}{1 + \varepsilon \cos \theta_2} \equiv \rho_2,$$

$$\left(\frac{z_1 - z_3}{z_1 + z_3}\right)^2 = \left(\frac{z_2 - z_4}{z_2 + z_4}\right)^2 = -\frac{1 - \cos(\theta_1 - \theta_2)}{1 + \cos(\theta_1 - \theta_2)} \equiv \sigma_{12}^{(-)},$$

$$\left(\frac{z_1 - z_4}{z_1 + z_4}\right)^2 = \left(\frac{z_2 - z_3}{z_2 + z_3}\right)^2 = -\frac{1 - \cos(\theta_1 + \theta_2)}{1 + \cos(\theta_1 + \theta_2)} \equiv \sigma_{12}^{(+)}. \quad (\text{A27})$$

The τ functions now become ($\alpha = 0, 1$)

$$\begin{aligned} \tau_\alpha = & 1 + (-1)^\alpha i [-2 \cotan \theta_1 e^{x \cos \theta_1} \sin(t \sin \theta_1) - 2 \cotan \theta_2 e^{x \cos \theta_2} \sin(t \sin \theta_2) + e^{\varepsilon x}] + e^{2x \cos \theta_1} + e^{2x \cos \theta_2} \\ & + 2\rho_1 \cotan \theta_1 e^{\varepsilon x} e^{x \cos \theta_1} \sin(t \sin \theta_1) + 2\rho_2 \cotan \theta_2 e^{\varepsilon x} e^{x \cos \theta_2} \sin(t \sin \theta_2) \\ & + 2\sigma_{12}^{(-)} \cotan \theta_1 \cotan \theta_2 e^{x(\cos \theta_1 + \cos \theta_2)} \cos[t(\sin \theta_1 + \sin \theta_2)] - 2\sigma_{12}^{(+)} \cotan \theta_1 \cotan \theta_2 e^{x(\cos \theta_1 + \cos \theta_2)} \cos[t(\sin \theta_1 - \sin \theta_2)] \\ & + (-1)^\alpha i \{-2 \cotan \theta_2 \sigma_{12}^{(+)} \sigma_{12}^{(-)} e^{x(2 \cos \theta_1 + \cos \theta_2)} \sin(t \sin \theta_2) + \rho_1^2 e^{2x \cos \theta_1} e^{\varepsilon x} - 2 \cotan \theta_1 \sigma_{12}^{(+)} \sigma_{12}^{(-)} e^{x(\cos \theta_1 + 2 \cos \theta_2)} \sin(t \sin \theta_1) \\ & + \rho_2^2 e^{2x \cos \theta_2} e^{\varepsilon x} + 2\sigma_{12}^{(-)} \rho_1 \rho_2 \cotan \theta_1 \cotan \theta_2 e^{\varepsilon x} e^{x(\cos \theta_1 + \cos \theta_2)} \cos[t(\sin \theta_1 + \sin \theta_2)] \\ & - 2\sigma_{12}^{(+)} \rho_1 \rho_2 \cotan \theta_1 \cotan \theta_2 e^{\varepsilon x} e^{x(\cos \theta_1 + \cos \theta_2)} \cos[t(\sin \theta_1 - \sin \theta_2)]\} + (\sigma_{12}^{(+)} \sigma_{12}^{(-)})^2 e^{2x(\cos \theta_1 + \cos \theta_2)} \\ & + 2\sigma_{12}^{(+)} \sigma_{12}^{(-)} \rho_1^2 \rho_2 \cotan \theta_2 e^{\varepsilon x} e^{x(2 \cos \theta_1 + \cos \theta_2)} \sin(t \sin \theta_2) + 2\sigma_{12}^{(+)} \sigma_{12}^{(-)} \rho_1 \rho_2^2 \cotan \theta_1 e^{\varepsilon x} e^{x(\cos \theta_1 + 2 \cos \theta_2)} \sin(t \sin \theta_1) \\ & + (-1)^\alpha i (\sigma_{12}^{(+)} \sigma_{12}^{(-)} \rho_1 \rho_2)^2 e^{\varepsilon x} e^{2x(\cos \theta_1 + \cos \theta_2)}. \quad (\text{A28}) \end{aligned}$$

This gives us the expression mentioned in Sec. III.

[1] G. Kälbermann, *J. Phys. A* **37**, 11603 (2004).
 [2] See e.g., A. C. Scott, *Nonlinear Science* (Oxford University Press, Oxford, 1999).
 [3] G. L. Lamb, Jr., *Elements of Soliton Theory* (Wiley-Interscience, New York, 1980).
 [4] L. P. Eisenhart, *A Treatise on the Differential Geometry of Curves and Surfaces* (Dover, New York, 1980).
 [5] O. Babelon, D. Bernard, and M. Talon, *Introduction to Classical Integrable Systems* (Cambridge University Press, Cambridge, U.K., 2003); L. D. Faddeev, in *Integrable Models in 1+1 Dimensional Quantum Field Theory*, edited by J. -B. Zuber and R. Stora, Proceedings of the Les Houches Summer School of Theoretical Physics, Session XXXIX, 1982 (Elsevier Science, Amsterdam, 1984); L. D. Faddeev and L. A. Takhtajan, *Hamiltonian Methods in the Theory of Solitons* (Springer, Berlin, 1986).
 [6] See, e.g., M. J. Ablowitz and P.A. Clarkson, *Solitons, Nonlinear Evolution Equations and Inverse Scattering* (Cambridge University Press, Cambridge, U.K., 1999).
 [7] C. R. Willis, *Phys. Rev. E* **73**, 068601 (2006).
 [8] N. G. Quintero, A. Sanchez, and F. G. Mertens, *Phys. Rev. E* **73**, 068602 (2006).
 [9] R. Boesch and C. R. Willis, *Phys. Rev. B* **42**, 2290 (1990).
 [10] N. G. Quintero, A. Sanchez, and F. G. Mertens, *Phys. Rev. E* **62**, R60 (2000).
 [11] R. Hirota, in *Solitons*, edited by R. K. Bullough and P. J. Caudrey (Springer, Berlin, 1980), pp. 157–176.
 [12] B. Piette and W. J. Zakrzewski, e-print arXiv:0710.4391.
 [13] L. A. Ferreira and W. J. Zakrzewski, *J. High Energy Phys.* (2007), 15.
 [14] D. I. Olive, N. Turok, and J. W. R. Underwood, *Nucl. Phys. B* **401**, 663 (1993).
 [15] H. Aratyn, C. P. Constantinidis, L. A. Ferreira, J. F. Gomes, and A. H. Zimmerman, *Nucl. Phys. B* **406**, 727 (1993).